time point reported was at 500 ms.

Acknowledgments

We thank Dr. Steven Robertson for the use of his computer program for the calculations of free calcium concentrations and Dr. Earl T. Wallick for valuable discussion. We also thank L. I. Tsai and M. G. Pease for technical assistance.

References

Froehlich, J. P., & Taylor, E. W. (1975) *J. Biol. Chem. 250*, 2013–2021.
Hicks, M. J., Shigekawa, M., & Katz, A. M. (1979) *Circ. Res. 44*, 384–391.
Inesi, E., Kurzmack, M., Coan, C., & Lewis, D. E. (1980) *J. Biol. Chem. 255*, 3025–3031.
Kirchberger, M. A., & Tada, M. (1976) *J. Biol. Chem. 251*, 725–729.
Kirchberger, M. A., Tada, M., & Katz, A. M. (1974) *J. Biol. Chem. 249*, 6166–6173.
Kirchberger, M. A., Tada, M., & Katz, A. M. (1975) *Recent Adv. Stud. Card. Struct. Metab. 5*, 103–115.
Kranias, E. G., Mandel, F., & Schwartz, A. (1980) *Biochem. Biophys. Res. Commun. 92*, 1370–1376.
Laemli, U. K. (1970) *Nature (London) 227*, 680–685.
LaRaia, P. J., & Morkin, E. (1974) *Circ. Res. 35*, 298–305.
Maizel, J. V., Jr. (1969) in *Fundamental Techniques in Virology* (Habel, K., & Salzman, J. P., Eds.) pp 334–362, Academic Press, New York.
Schwartz, A., Entman, M. L., Kaniike, K., Lane, L. K., Van Winkle, W. B., & Bornet, E. P. (1976) *Biochim. Biophys. Acta 426*, 57–72.
Sillen, L. G., & Martell, A. E. (1964) in *Stability Constants of Metal-Ion Complexes*, 2nd ed., Ser. Publ. No. 17, The Chemical Society, Burlington House, London, WIV OBN.
Sumida, M., Wang, T., Mandel, F., Froehlich, J. P., & Schwartz, A. (1978) *J. Biol. Chem. 253*, 8772–8777.
Sumida, M., Wang, T., Schwartz, A., Younkin, C., & Froehlich, J. P. (1980) *J. Biol. Chem. 255*, 1497–1503.
Tada, M., Kirchberger, M. A., Repke, D. I., & Katz, A. M. (1974) *J. Biol. Chem. 249*, 6174–6180.
Tada, M., Kirchberger, M. A., & Katz, A. M. (1975) *J. Biol. Chem. 250*, 2640–2647.
Tada, M., Yamamoto, T., & Tonomura, Y. (1978) *Physiol. Rev. 58*, 1–79.
Tada, M., Ohmori, F., Yamada, M., & Abe, H. (1979) *J. Biol. Chem. 254*, 319–326.
Tada, M., Yamada, M., Ohmori, F., Kuzuya, T., Inui, M., & Abe, H. (1980) *J. Biol. Chem. 255*, 1985–1992.
Weber, K., & Osborn, M. (1969) *J. Biol. Chem. 244*, 4406–4412.
Weller, M., & Laing, W. (1979) *Biochim. Biophys. Acta 551*, 406–419.
Will, H., Blanck, J., Smettan, G., & Wollenberger, A. (1976) *Biochim. Biophys. Acta 449*, 225–303.
Wray, H. L., & Gray, R. R. (1977) *Biochim. Biophys. Acta 461*, 441–459.

Quantitative Analyses of Calcium-Induced Spectral Changes in Extrinsic Cotton Effects of Cobalt-Substituted Concanavalin A†

Alan D. Cardin,‡ W. David Behnke,* and Frederic Mandel

ABSTRACT: The visible cobalt circular dichroism (CD) of cobalt-substituted concanavalin A (Con A) is highly sensitive to Ca^{2+}-induced conformational changes that occur in the metal binding region. The observed ellipticity is separately resolved into discrete conformational spectra with separate extrinsic bands. The conformational forms of the metal region are further delineated on the basis of their differential spectral response to the competitive removal of metals by ethylenediaminetetraacetic acid (EDTA). The spectral forms sensitive to the effects of EDTA, cobalt–Con A (CPS, $\epsilon_{CPS}^{470} = 215$ M^{-1}) and calcium–cobalt–Con A (CaCPS, $\epsilon_{CaCPS}^{470} = 141$ M^{-1}), exhibit both unique extinctions and band shapes in the 400–600-nm region, as does the fully metalized EDTA-resistant species CaCPR ($\epsilon_{CaCPR}^{470} = 54$ M^{-1}). Equations describing the time dependence of the observed ellipticity have been derived in terms of the kinetic scheme, CPS + Ca ⇋ CaCPS ⇋ CaCPR, in which the second equilibrium is slow compared to the first. The above assignments allow a more complete quantitative description of the changes in CD amplitudes and band shapes due to Ca^{2+} binding and thus facilitate the understanding of Ca^{2+} interactions. Calcium binds to 0.93 Ca^{2+} site/25 500 M_r in CaCPS with a K_d for Ca^{2+} = 2.1×10^{-3} M at pH 5.3 and 25 °C. The interaction of Ca^{2+} with CPS to form CaCPS occurs at two equivalent and noninteracting S_2 sites each present on separate subunits of the Con A dimer. Furthermore, the rate constant describing the rate of formation of CaCPR was determined.

Concanavalin A (Con A), a metallolectin isolated from the Jack bean *Canavalia ensiformis* (Sumner & Howell, 1936), has a substrate specificity for carbohydrate structures bearing the D-arabinopyranoside configuration (Goldstein et al., 1965, 1973). This protein has been the subject of numerous biochemical studies owing primarily to its ability to bind certain cell-surface carbohydrate acceptors although its true biological function is not known (Bittiger & Schnebli, 1976; Lis & Sharon, 1973). Among the many interesting effects induced by Con A binding is its ability to agglutinate selectively different cell types (Inbar & Sachs, 1969) and to elicit a mitogenic response in lymphocytes (Beckert & Sharkey, 1970; Powell & Leon, 1970; Wecksler et al., 1968).

The metal binding region of Con A has been a subject of particular interest, as it has a structural relation to the region where saccharides are bound. Each protomeric unit of Con

† From the Department of Biological Chemistry (A.D.C. and W.D.B.) and the Department of Pharmacology and Cell Biophysics (F.M.), University of Cincinnati College of Medicine, Cincinnati, Ohio 45267. *Received March 3, 1980.* Supported in part by the National Institutes of Health (HL 23741).

‡ In partial fulfillment of the degree Doctor of Philosophy.

0006-2960/80/0419-5439$01.00/0

A (25 500) contains two distinct metal binding sites, classically designated as S_1 and S_2. The crystal structure of these two sites has been determined by X-ray crystallographic studies (Edleman et al., 1972; Hardman & Ainsworth, 1972) and can be described as a binuclear complex of two polyhedrons sharing a common edge (Reeke et al., 1974). The S_1 and S_2 metals are separated by 4.5 Å, and each metal ion shares Asp-10 and -19 as metal ligands. Some other residues important to metal chelation include Glu-8 (S_1), His-24 (S_1), Asp-208 (S_2), Arg-228 (S_2), and Tyr-12 (S_2). The S_1 metal site shows a specificity primarily for divalent cations having an affinity for nitrogen ligands (e.g., Co^{2+}, Mn^{2+}, Zn^{2+}, and Ni^{2+}) while site S_2 exhibits a high specificity for Ca^{2+}. Recent studies have indicated that under certain conditions Mn^{2+} may activate Con A by binding both S_1 and S_2 (Brown et al., 1977; Koenig et al., 1978) while other studies, utilizing similar conditions, contend that Mn^{2+} is bound to a single hybrid site instead (Christie et al., 1979).

Our primary interest is to understand the mechanism of the Ca^{2+}-induced refolding process of the Con A polypeptide structure initiated through site S_2. Our ultimate goal is to resolve changes in solution structure which occur as a result of Ca^{2+} binding and to relate these changes at the atomic level to a structural mechanism explaining formation of the substrate site. To such end, we have exploited the optical probe Co^{2+}, bound to S_1, to study the Ca^{2+}-induced refolding process and to elucidate the structural mechanism involved in the generation of the native structure. Two structural perturbations modulate the extrinsic Co^{2+} bands: (1) Ca^{2+} binding to S_2 and (2) a slow time-dependent protein structural change which occurs at S_1 following Ca^{2+} binding. The observed Co^{2+} circular dichroic (CD) transitions can be resolved into simpler bands and assigned to discrete conformational forms.

This report deals primarily with the methods required for spectral band shape assignments, the quantitative aspects of Ca^{2+} binding, and the refolding process which occurs subsequent to Ca^{2+} binding. Spectral assignments in the visible Co^{2+} region now facilitate resolution into discrete Gaussian components. Further assignments of these components to changes in specific metal–ligand interactions are under way and will constitute the subject of a future report.

In addition, these studies complement further the understanding of changes which occur in the intrinsic structural properties of the protein (Cardin et al., 1979), since, like the present study, both Co^{2+} and Ca^{2+} were utilized.

Materials and Methods

Concanavalin A was prepared according to the procedure of Agrawal & Goldstein (1967) from jack bean meal (Pfaltz and Bauer, Inc.). The isolated protein was found to be homogeneous, according to the following criteria: sedimentation velocity, sedimentation equilibrium, discontinuous polyacrylamide gel electrophoresis, and amino acid composition. With the buffer conditions employed, concanavalin A exists exclusively in its dimeric form with a molecular weight of 55 000. This was verified by meniscus-depletion ultracentrifugation techniques (Yphantis, 1964).

Apoconcanavalin A was prepared by dissolving 1.0 g of protein in 30 mL of distilled water. HCl (1 M) was then added slowly with stirring to a final pH of 1.2. After 45 min at 25 °C, the solution was transferred to thoroughly rinsed dialysis bags (which were previously boiled in a 5% $NaHCO_3$–1 mM ethylenediaminetetraacetic acid (EDTA) solution) and subjected to dialysis against four 6-L changes of double glass distilled water at 4 °C, followed by exhaustive dialysis against 0.1 M $NaC_2H_3O_2$–$HC_2H_3O_2$ and 0.9 M NaCl, pH 5.2, buffer.

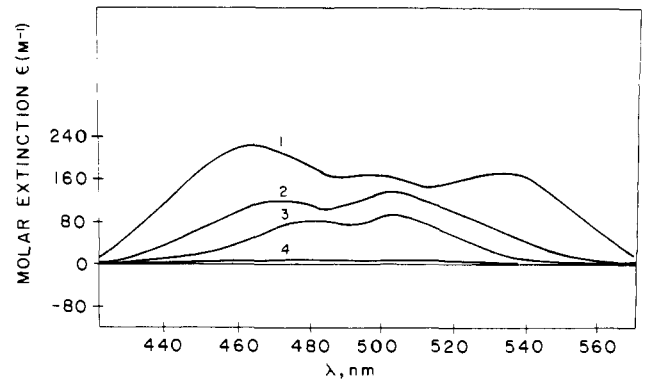

FIGURE 1: The visible CD spectrum of three different metal–protein complexes: (1) cobalt–Con A, [CPS] = 1.1×10^{-3} M at 2 °C; (2) calcium–cobalt–Con A, [CaCPS] = 1.1×10^{-3} M at three different final calcium concentrations and at two different temperatures ([Ca^{2+}] = 0.21, 0.31, and 0.75 M and temperatures = 2 and 25 °C); (3) the CaCPR form, [CaCPR] = 1.1×10^{-3}, which results following a temperature shift from 2 °C of (2) to 25 °C for 4 h ([Ca^{2+}] = 0.75 M); (4) the visible CD spectrum of sample 2 at 2 °C following the addition of EDTA ([EDTA] = 0.45 M). In each case, ϵ represents the observed ellipticity, Θ_{obsd}, divided by the total protein concentration, $[P]_T = 1.1 \times 10^{-3}$ M.

Protein concentrations were determined spectrophotometrically at pH 5.2 by using an extinction coefficient ($\epsilon_{280nm}^{0.1\%}$) of 1.24 (Yariv et al., 1968).

The analytical grade reagents used in preparing buffers were purchased from Mallinckrodt, Inc. Buffers were dithizone extracted to remove heavy metal ion contaminants and then subjected to spectrographic analyses. Further precautions against adventitious metal ion contamination were employed according to Thiers (1957). Stock solutions of cobalt and calcium were prepared approximately 0.1–0.2 M in glass-distilled water and standardized by atomic absorption analyses. All metal salts were of spectrographic quality and were obtained from Apache Chemicals, Inc.

CD spectra were obtained with a Cary 61 spectropolarimeter. Standardization of the instrument was accomplished by using a 1 mg/mL aqueous solution of *d*-10-camphorsulfonic acid as specified by Varian Associates. Cells with 1.0-cm path lengths were utilized for all spectral measurements. Molar extinctions expressed in units of M^{-1} were determined by dividing the observed ellipticity by the appropriate concentration of each protein species. Ellipticity may be converted to units of degrees by multiplying the observed ellipticity by the full-range factor, 0.02.

Results

The binding of cobalt to demetalized concanavalin A generates a characteristic CD spectrum in the visible region. Three major bands are generated with maxima centered at 470, 505, and 530 nm (curve 1 of Figure 1). These bands arise from the binding of cobalt to the apoprotein and are not due to the free ion (Kalb & Pecht, 1973). Even at very low [Co^{2+}]/[P] ratios, the general overall band shape is identical with that obtained at saturating [Co^{2+}]/[P] ratios.

The addition of competing metals such as Mn^{2+}, Zn^{2+}, and Ni^{2+} decreases the amplitude of the cobalt spectrum without affecting the overall band shape (not shown) while the addition of excess EDTA completely and rapidly abolishes the extrinsic Co^{2+} band. These data illustrate that (1) Co^{2+} binds to the same site as Mn^{2+}, Zn^{2+}, and Ni^{2+} and (2) this spectral form is highly sensitive to the competitive removal of Co^{2+} by EDTA. Thus, the band shape depicted by curve 1 of Figure 1 is definitive for Co^{2+} bound to the S_1 site of apo-Con A. This

Table I: Band Maxima and Spectral Extinctions for Several Metal–Con A Complexes[a]

species	maxima (nm)	extinctions (M^{-1})
CPS	470, 505, 530	225 (208),[b] 171, 182
CaCPS	475, 505, 525	134 (120),[c] 118, 130
CaCPR	483, 505	80, 91

[a] All data may be converted to units of deg·M^{-1} by multiplying by 0.02 (2 °C, pH 5.3). [b] The measured extinction at 26.7 °C. [c] The measured extinction at 34.5 °C.

particular metal–protein complex will be denoted as CPS to signify a cobalt form whose spectral properties are sensitive to metal chelation by EDTA.

Calcium binding to CPS causes a rapid reduction in CD spectral amplitude which occurs at all wavelengths. This effect is complete within the mixing time of the experiment (4–5 s). The magnitude of the Ca^{2+}-induced reduction is a function of the Ca^{2+}-concentration and is a saturable process. Curve 2 of Figure 1 illustrates the CD spectrum generated within the experimental mixing time when saturable amounts of Ca^{2+} are added (e.g., in the $[Ca^{2+}]/[CPS]$ ratio range > 190). This spectrum exhibits two prominent maxima, one at 473 nm and a second at 505 nm.

The spectra illustrated in Figure 1 were recorded at 2 °C. Within the investigated temperature range of 2–25 °C, the generation of curve 2 occurs during the mixing time of the experiment and thus essentially is independent of temperature. The half-life of the CaCP species represented by curve 2 is, however, highly temperature dependent. At 2 °C, this high-extinction CaCP form (curve 2) slowly evolves to a CaCP form of lower extinction over a period of a few hours (curve 3). After this time period further time-dependent changes in spectral amplitude and band shape do not occur. At 25 °C, curve 2 is less stable kinetically and will evolve into curve 3 within 30 min. Table I lists the prominent band positions and relative extinctions of each metal–Con A complex.

A further delineation between the two CaCP species can be made on the basis of differential spectral responses to EDTA. If a 40-fold molar excess of EDTA to total $[Co^{2+}]$ is added to the Ca^{2+} form represented by curve 2 of Figure 1, protein-bound Co^{2+} is rapidly sequestered as evidenced by the complete loss of all spectral intensity in the visible region. Calcium is also removed from the CaCP form as a readdition of Co^{2+} in excess of the EDTA concentration generates a spectrum characteristic of CPS rather than either of the two CaCP forms. Thus, cobalt and calcium are rapidly removed from both CPS and the high-extinction CaCP form within the mixing time of the experiment. In contrast, the spectral band characteristic of the low-extinction Ca^{2+} form (curve 3) remains stable for several hours following the addition of EDTA. Those forms which exhibit spectral *sensitivity* to the effects of EDTA are thus denoted with an S, e.g., CPS and CaCPS. Alternatively, the low-extinction CaCP form is denoted as CaCPR in which the symbol R signifies spectral resistance to EDTA.

Figure 2 illustrates the time-dependent changes that occur at 470 nm when Ca^{2+} is added to CPS. This wavelength was chosen because it represents the spectral region which exhibits the largest amplitude change and thus allows for the maximum resolution of the observed kinetic events. Calcium binding to CPS elicits two distinct spectral responses in the visible region which are well separated in time (Cardin et al., 1978). First, an initial rapid-phase reduction in molar extinction occurs with essentially no time delay relative to the resolving time of the measurement. Second, this initial phase is followed by a slow-phase reduction in ellipticity. The rapid-phase reduction is representative of CaCPS production (curve 2 of Figure 1), and the slow-phase reduction is characteristic of CaCPR production (curve 3 of Figure 1). The experiment illustrated in Figure 2 shows a slow-phase reduction with a total duration of ~25 min at 26.7 °C. Both kinetic effects, the rapid-phase and the slow-phase reduction, exhibit a notable $[Ca^{2+}]$ dependence, and each process is saturable.

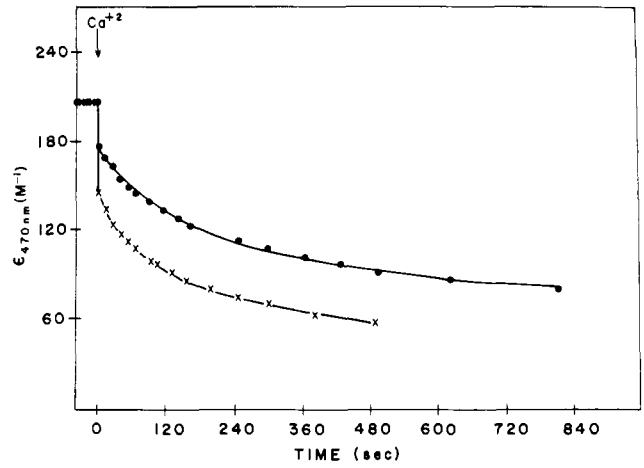

FIGURE 2: The calcium concentration dependence upon both fast and slow spectral reductions monitored at a single wavelength, 470 nm. Initial [CPS] = 1.0×10^{-3} M; $[Ca^{2+}] = 1.3 \times 10^{-3}$ M (●); $[Ca^{2+}] = 3.4 \times 10^{-3}$ M (×); pH 5.3; 26.7 °C. Here, $\epsilon = \Theta_{obsd}/[P]_T$.

Scheme I

$$\underset{(\epsilon = 215\ M^{-1})}{CPS} + Ca^{2+} \underset{k_{-1}}{\overset{k_1}{\rightleftharpoons}} \underset{(\epsilon = 141\ M^{-1})}{CaCPS} \underset{k_{-2}}{\overset{k_2}{\rightleftharpoons}} \underset{(\epsilon = 54\ M^{-1})}{CaCPR}$$

At saturable Ca^{2+} concentrations (>0.05 M), where maximization of the rate of the slow-phase amplitude change occurs, the magnitude of the spectral change from curve 2 to curve 3 of Figure 1 is not easily quantitated since it accounts for only 20–30% of the total amplitude of curve 1. However, at low [Ca], the spectral change represents a larger fraction of the total amplitude. Thus, for maximal resolution of the time dependence, studies in the visible CD region were conducted at low calcium concentrations.

Quantitative Considerations

Rapid-Phase Spectral Reduction. The two spectral phases elicited by Ca^{2+} binding are well separated in time, and each phase can be studied independently. We have assigned the rapid-phase reduction to the first equilibrium of Scheme I. As the binding event between Ca^{2+} and CPS triggers the slow-phase process of protein activation, it is of interest to understand the mechanism(s) by which rapid binding of Ca^{2+} is able to drive the slow conformational reaction. To date, the number of Ca^{2+} sites involved in this interaction has not been resolved. On the basis of the assignments, the first equilibrium of Scheme I can be studied directly.

Under conditions of full S_1 occupancy by Co^{2+}, the ellipticity in the visible CD region is given as

$$\Theta_{CPS} = \epsilon_{CPS}[CPS]_0 \quad (1)$$

where $[CPS]_0 = [P]_T$, the total protein concentration, and ϵ is the molar extinction coefficient. Upon the addition of Ca^{2+}, the CD amplitude is given by eq 2, which assumes a 1:1

$$\Theta_{obsd} = \epsilon_{CPS}[CPS] + \epsilon_{CaCPS}[CaCPS] \quad (2)$$

binding stoichiometry and in which the concentration of CPS at any time is $[CPS] = [P]_T - [Ca^{2+}]_b$, where $[Ca^{2+}]_b$ rep-

resents the concentration of bound calcium. Thus, it can be shown that the spectral jump induced by Ca^{2+} binding is given by eq 3 where $\Delta\epsilon = \epsilon_{CPS} - \epsilon_{CaCPS}$ is constant. The addition

$$\Delta\Theta(\text{jump}) = [Ca^{2+}]_b\Delta\epsilon \quad (3)$$

of EDTA immediately following the initial Ca^{2+} addition to CPS results in essentially no amplitude contribution attributable to CaCPR formation (Figure 1, curve 4). Thus, the amount of Ca^{2+} bound to site S_2 is equal to [CaCPS] and can be determined from eq 3. A Scatchard (1949) plot of a typical experiment in which the magnitude of the rapid-phase reduction is measured as a function of the total calcium concentration, $[Ca^{2+}]_T$, is shown in Figure 3. As can be seen, a K_d for Ca^{2+} of 2.1×10^{-3} M is obtained, and extrapolation yields 0.93 mol of Ca^{2+} bound at S_2 per mol of CPS. It is at this stoichiometry of bound Ca^{2+} to CPS that we observe the complete conversion of CPS to the final active form, CaCPR. Additional Ca^{2+} sites of lower affinity, if present, are not detectable within the limits of resolution of the current measurement and are not involved in the Ca^{2+}-induced reactivation of the protein at pH 5.3. We have found, however, that data cast in the form of a Scatchard plot in which a time factor contributes to the magnitude of the observed ellipticity (CaCPR production in addition to the CaCPS formed) results in a curvilinear plot. This is expected as multiple species are present which interact with Ca^{2+} at the same site but with varying affinities. The Ca^{2+} binding data analyzed in terms of a Hill plot (Van Holde, 1973) yield a Hill coefficient of 0.94. When the data are analyzed according to the method of Tanford (1967), it is found that up to a fractional occupancy of 0.7 Ca^{2+} ion/subunit, no significant interaction occurs to indicate a cooperative behavior between the separate Ca^{2+} sites located on each subunit of the Con A dimer. These data support a noncooperative model for calcium binding to CPS.

Time and Ca^{2+} Dependence of Reaction Intermediates. The time-dependent concentrations of CPS, CaCPS, and CaCPR are given by eq 4–6 where K^* and K' represent the fractional

$$[CPS] = K^*[P]_T e^{-k_{obsd}t} \quad (4)$$

$$[CaCPS] = K'[P]_T e^{-k_{obsd}t} \quad (5)$$

$$[CaCPR] = [P]_T(1 - e^{-k_{obsd}t}) \quad (6)$$

distribution of CPS and CaCPS, respectively, at equilibrium (note that $K^* + K' = 1$) and are given by eq 7 and 8. In the

$$K^* = K_d/(K_d + [Ca^{2+}]_f) \quad (7)$$

$$K' = [Ca^{2+}]_f/(K_d + [Ca^{2+}]_f) \quad (8)$$

limit of high calcium concentrations, $K^* \rightarrow 0$ and $K' \rightarrow 1$. The observed rate constant, k_{obsd}, is a function of the [CaCPS] and is given by eq 9 where k_2 is the intrinsic rate constant for the

$$k_{obsd} = K'k_2 \quad (9)$$

CaCPS → CaCPR conversion. Note that in the limit of high $[Ca^{2+}]$, $k_{obsd} = k_2$ and [CPS] = 0.

Interpretation of Slow-Amplitude CD Change. The *observed* CD amplitude in the visible region can be expressed as the sum of the elliptical contributions of the three species present. If each of the species in eq 4–6 is multiplied by their respective extinctions, the observed ellipticity is given by

$$\Theta_{obsd} = [P]_T[Ie^{-k_{obsd}t} + \epsilon_{CaCPR}] \quad (10)$$

where

$$I = K^*\epsilon_{CPS} + K'\epsilon_{CaCPS} - \epsilon_{CaCPR} \quad (11)$$

Thus, a semilogarithmic plot of the quantity $\Theta_{obsd}/[P]_T - \epsilon_{CaCPR}$ vs. time should be linear with slope equal to $k_{obsd}/2.303$ and an intercept given by eq 11. Figure 4 shows the data at three calcium concentrations. The calcium dependence of the observed rates and intercepts is described by eq 7–9. As the $[Ca^{2+}]$ is increased, the values of k_{obsd} increase and the intercepts converge. A 2.5-fold increase in the total calcium concentration results in a factor of 2.3 increase in k_{obsd}, whereas a factor of 7.2 increase in $[Ca^{2+}]_T$ results in a factor of 2.8 increase in k_{obsd}. The observed 2.3- and 2.8-fold increases in k_{obsd} can be compared respectively to the theoretical increases in k_{obsd} of 1.9 and 3.0 computed from eq 8 and 9, based on K_d for Ca^{2+} of 2.1×10^{-3} M (Figure 3). Furthermore, as is

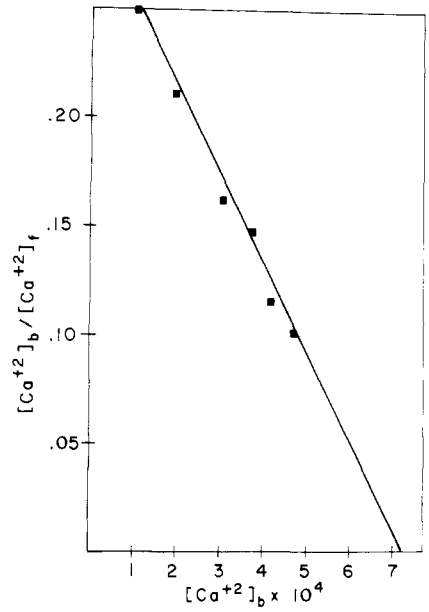

FIGURE 3: Scatchard plot (1949) for Ca^{2+} binding representing equilibrium 1 of Scheme I. Computations for the amount of bound Ca^{2+} were based on the magnitude of the fast-phase amplitude reduction at 470 nm. The experiment was performed at 25 °C and pH 5.3. [CPS] = 7.74×10^{-4} M and the intercept, 7.20×10^{-4} M.

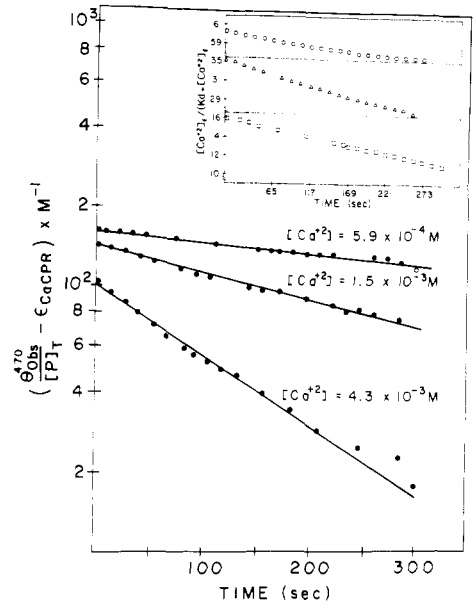

FIGURE 4: This figure illustrates a semilogarithmic plot of the observed ellipticity according to eq 10 of the text. The equation takes into account the presence of CPS, CaCPS, and CaCPR. From these data the values of k_{obsd} were determined. (Inset) These data illustrate the computed values of K' as a function of $[Ca^{2+}]_T$. With the exception of $[Ca^{2+}]_f$, all constants were experimentally determined. $[Ca^{2+}]_f$ was determined by computer iteration. $[Ca^{2+}]_T$: (○) 4.3×10^{-3} M; (△) 1.5×10^{-3} M; (□) 5.9×10^{-4} M.

Table II: Effect of $[Ca^{2+}]$ upon the Value of the Observed Rate Constant for the CaCPS → CaCPR Conversion at 25 °C and pH 5.3

method of analysis	$[Ca^{2+}]$ (M)	k_{obsd} $(s^{-1})^a$	k $(s^{-1})^b$
$\Theta_{obsd}/[P]_T - \epsilon_{CaCPR}$	5.9×10^{-4}	8.9×10^{-4a}	$(6.8 \pm 0.2) \times 10^{-3a}$
$\Theta_{obsd}/[P]_T - \epsilon_{CaCPR}$	1.5×10^{-3}	2.1×10^{-3a}	$(7.8 \pm 0.1) \times 10^{-3b}$
$\Theta_{obsd}/[P]_T - \epsilon_{CaCPR}$	4.3×10^{-3}	5.8×10^{-3a}	$(9.1 \pm 0.2) \times 10^{-3b}$

[a] The observed rates were obtained from the $\Theta_{obsd}/[P]_T - \epsilon_{CaCPR}$ vs. t plots. [b] Values for the intrinsic rates were obtained from $\Theta_{obsd}/[P]_T - \epsilon_{CaCPR}$ vs. $K't$ plots.

evident from eq 7–11, the intercept should decrease with increasing $[Ca^{2+}]$ as is observed. Ultimately at saturating $[Ca^{2+}]$ the intercept converges to $\epsilon_{CaCPS} - \epsilon_{CaCPR}$ (e.g., 66 M^{-1}; see Figure 1).

The effect of Ca^{2+} upon the visible CD ellipticity can be understood by studying the individual terms in eq 10 and 11. The production of CaCPR lowers the free calcium concentration which in turn affects the values of K^* and K'. Thus, at any given time t, Θ_{obsd} will be weighted by the appropriate values of K^* and K'. However, from eq 9–11 it can be seen that although I is a function of both K^* and K', the observed rate constant, k_{obsd}, is a function of K' only. Thus, the computation of K' at each time point will allow the value of k_2 to be determined. An iterative computer program was written and used to determine the free calcium concentration and K' at any given time. The inset of Figure 4 illustrates the variation of K' as a function of $[Ca^{2+}]_T$. As seen, K' varies almost linearly with the free $[Ca^{2+}]$. At $[Ca^{2+}]_T = 4.3 \times 10^{-3}$ M, K' is observed to vary only 5% over the projected time range while at $[Ca^{2+}]_T = 1.5 \times 10^{-3}$ M and 5.9×10^{-4} M, K' varies by 19% and 31%, respectively.

The experimentally determined values of the extinctions of each species, the total protein concentration, and the K_d for Ca^{2+} were treated as constants. For each value of Θ_{obsd}, the $[Ca^{2+}]_T$ was used to initialize the iteration, and at each time increment the values for free calcium, K', [CPS], [CaCPS], and [CaCPR] were determined. Semilogarithmic plots of the quantity $\Theta_{obsd}/[P]_T - \epsilon_{CaCPR}$ vs. $K't$ were found to be linear at the same three calcium concentrations as those of Figure 4. The values of k_2 and k_{obsd} at three different calcium concentrations are listed in Table II. The average value for k_2 is 7.9×10^{-3} s^{-1} which is in excellent agreement with previously determined values for this rate constant (Brown et al., 1977; Sherry et al., 1978; Cardin et al., 1979). The ~15% variation in k_2 can be reduced to <5% if the extinctions for CPS, CaCPS, and CaCPR and the value of K_d for calcium are allowed to vary 5–8% (within experimental error) from their experimentally determined values.

Figure 5 illustrates the variation in each population of metallo species as a function of time (eq 5–10). It should be noted that these calculations (using the iterative computer program) do not assume that the [CaCPS] remains constant but do show that the concentration of CaCPS only varies a few percent over the time investigated (0–300 min).

Discussion

The spectra illustrated in Figure 1 demonstrate a minimum of three different metal–Con A conformations. These forms, which can be spectrally observed, are representative of different structural forms of the metal binding region. The CPS and the two CaCP conformers can be differentiated on the basis of spectral band shapes, amplitude, and spectral responses to

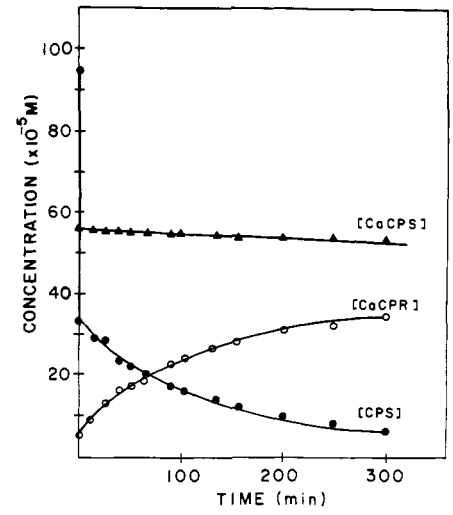

FIGURE 5: This figure illustrates the variation in molar concentrations of species after the addition of Ca^{2+} to CPS at 5 °C. Initial concentration of [CPS] = 9.5×10^{-4} M. For normalization purposes, the initial time point ($t = 0$) shown in this figure represents an actual elapsed time of 5 min after the addition of calcium.

EDTA. From these data it was possible to show that Ca^{2+} binds to CPS at a single site to yield the EDTA-sensitive form, CaCPS, characterized by a K_d for $Ca^{2+} \simeq 2 \times 10^{-3}$ M. Moreover, the binding of Ca^{2+} occurs in a noncooperative fashion when apo-Con A is preincubated with Co^{2+}. Alter et al. (1977) and Alter & Magnuson (1979) have investigated an alternate pathway for the metal ion induced refolding process from pH 5.1 to 6.45 in which the apoprotein is first preincubated with Ca^{2+} before the addition of Mn^{2+}. These investigators have provided evidence for a model in which a single Mn^{2+} ion binds to the first subunit of the Con A dimer. This interaction is responsible for a reduced binding rate (their rate-limiting step) for the association of the second Mn^{2+} ion to the remaining unoccupied subunit of the Con A dimer. Following the association of the second Mn^{2+} ion, a rapid structural isomerization occurs to yield a protein with the characteristics of the native structure. It is clear from their data that even at low pH (pH 5.1) substantial cooperativity exists for the binding of the second Mn^{2+} ion (Alter et al., 1977). Recently Koenig et al. (1978) have investigated the kinetics of Mn^{2+} association to apo-Con A preincubated with Ca^{2+} at pH 6.4 in which a cooperative binding mechanism for Mn^{2+} was not observed. The data of Koenig et al. (1978) have been analyzed in terms of a competitive binding mechanism in which Mn^{2+} displaces Ca^{2+} from their CaCaPL structure. It is clear that Ca^{2+} can yield an active structure in the absence of added S_1 metal (Richardson & Behnke, 1976; Harrington & Wilkins, 1978; Koenig et al., 1978). The data of Koenig et al. (1978) reflect Mn^{2+} binding to an end product of the reaction scheme (the final equilibrium or locked form, CaCaPL) while the data of Alter et al. (1977) and Alter & Magnuson (1979) reflect Mn^{2+} binding not to a locked form, but rather to a preequilibrium form which appears earlier in its reaction pathway. It should be emphasized that our current data yield different information from either that of Alter et al. (1977), Alter & Magnuson (1979), or Koenig et al. (1978) on at least three accounts: (1) a different reaction pathway is utilized, (2) the binding of Ca^{2+} is being followed and not Mn^{2+} (or Co^{2+}), and (3) the metal binding properties of a single metallo form, CaCPS, is being characterized.

The slow-phase change in ellipticity which occurs in the visible region indicates the rate at which active protein is formed (Cardin & Behnke, 1978). The spectral responses

generated in the near-UV CD region by Ca^{2+} binding are modulated by a sensitive tyrosyl residue apparently located in or near the metal binding region (Cardin et al., 1979). The slow conformational change monitored in the near-UV CD occurs with a forward rate constant of $\sim 1 \times 10^{-2}$ s^{-1} at 25 °C. This value compares favorably with the value of $\sim 8 \times 10^{-3}$ s^{-1} as sensed by the optically active Co^{2+} ion. New information of the current study includes the observation that the conformational differences measured in the visible region can be localized exclusively to the metal region and, more specifically, to sites S_1 and S_2. Thus, our previous notion that tertiary structural rearrangements in the vicinity of the metal region may comprise the rate-limiting motions is consistent both qualitatively and quantitatively with measurements made in the visible CD region. Doyle et al. (1975) and Stroupe & Doyle (1980), using UV difference absorption spectroscopy, found that these measurements are also sensitive to Ca^{2+}-induced tertiary structural changes involving tyrosine, tryptophan, and possibly phenylalanine and histidine. Although these investigators are not able to assign these structural changes to a localized region, these structural changes occur with a forward rate constant of 1.2×10^{-2} s^{-1}. As such, equating a 22 kcal/mol barrier to a single isomerization event in a peptide bond (Brown et al., 1977) does not yield a satisfactory explanation relating the mechanism of Ca^{2+}-induced structural changes during activation. Crystallographic evidence does show that the major structural changes between crystals of native and demetalized Con A are confined primarily to the region where metals are bound (Reeke et al., 1978; Shoham et al., 1979). Side-chain motions important to saccharide binding and the structural disposition of the peptide bond at residue 207 are points of interest awaiting further clarification by crystallographic studies.

Summary

The optical probe Co^{2+} bound at S_1 reports events which occur in the metal region. Two generalized structural perturbations affecting Co^{2+} are resolved: (1) Ca^{2+} binding to S_2 and (2) the slow time-dependent protein structural changes which occur at S_1 induced by Ca^{2+} binding.

In the presence of Ca^{2+}, the observed visible CD absorption bands of cobalt-substituted concanavalin A represent contributions from three distinct metallo forms, CPS, CaCPS, and CaCPR. Each form is characterized by unique extinctions and band shapes. The species CPS and CaCPS are further differentiated from CaCPR based on their spectral sensitivity to EDTA. The equilibrium between CPS and CaCPS occurs rapidly. Calcium binds to each S_2 site of the Con A dimer in a noncooperative fashion with a K_d for $Ca^{2+} \simeq 2 \times 10^{-3}$ M. The conformational conversion from an EDTA-sensitive to an EDTA-resistant form occurs with a forward rate constant of $\sim 8 \times 10^{-3}$ s^{-1} at 25 °C. Upon Ca^{2+} binding, the optically active probe, Co^{2+}, is sensitive to changes in metal coordination chemistry which comprise a structural feature of the mechanism involved in activation. These changes occur with the same time constant as those observed in the near-UV CD region suggesting that structural changes in aromatic side-chain residues located in or near the vicinity of the metal region also comprise a structural feature important to the mechanism which relates metal binding to substrate binding.

Appendix

The proposed model can be represented by Scheme I in which $k_2 \gg k_{-2}$ and where the first equilibrium is considered to be rapid compared to the second (fast-phase spectral reduction vs. the slow-phase spectral reduction). The differential equation describing Scheme I is given by eq A1. The assumption of fast equilibrium between [CaCPS] and [CPS] can be represented by eq A2 where $[Ca^{2+}]_f$ is the free calcium concentration and K_d is the dissociation constant for CaCPS. By use of the fact that P_T = [CPS] + [CaCPS] + [CaCPR], eq A2 can be rewritten as

$$\frac{d[CaCPR]}{dt} = k_2[CaCPS] \quad (A1)$$

$$[CaCPS] = [Ca^{2+}]_f[CPS]/K_d \quad (A2)$$

$$[CaCPS] = \frac{[Ca^{2+}]_f}{K_d + [Ca^{2+}]_f}([P]_T - [CaCPR]) \quad (A3)$$

Substituting the expression for [CaCPS] of eq A3 into eq A1 and integrating yields

$$\ln\left(\frac{[P]_T}{[P_T] - [CaCPR]}\right) = k_{obsd}t \quad (A4)$$

where

$$k_{obsd} = k_2\frac{[Ca^{2+}]_f}{K_d + [Ca^{2+}]_f} \quad (A5)$$

thus

$$[CaCPR] = [P]_T(1 - e^{-k_{obsd}t}) \quad (A6)$$

Substituting this expression for [CaCPR] in eq A3 yields eq A7. Solving eq A2 for CPS in terms of CaCPS yields eq A8.

$$[CaCPS] = \{[Ca^{2+}]_f/(K_d + [Ca^{2+}])\}[P]_Te^{-k_{obsd}t} \quad (A7)$$

$$[CPS] = \{K_d/(K_d + [Ca^{2+}]_f)\}[P]_Te^{-k_{obsd}t} \quad (A8)$$

In the visible region of the CD, each species will generate a contribution to the measured amplitude and can be described by eq A9 where Θ_A, ϵ_A, and [A] represent, respectively, the amplitude contribution of species A to the visible CD region, the molar extinction of A, and the concentration of species A. The observed amplitude then is given by eq A10 at any time following Ca^{2+} addition. Thus, by virtue of the expressions for the time-dependent concentrations of [CPS], [CaCPS], and [CaCPR] derived above, it can be shown that

$$\Theta_A = \epsilon_A[A] \quad (A9)$$

$$\Theta_{obsd} = \epsilon_{CPS}[CPS] + \epsilon_{CaCPS}[CaCPS] + \epsilon_{CaCPR}[CaCPR] \quad (A10)$$

$$\Theta_{obsd} = [P]_T[\epsilon_{CaCPR} + e^{-k_{obsd}t}(\epsilon_{CPS}K^* + \epsilon_{CaCPS}K' - \epsilon_{CaCPR})] \quad (A11)$$

Thus

$$\Theta_{obsd}/[P_T] - \epsilon_{CaCPR} = Ae^{-k_{obsd}t} \quad (A12)$$

where

$$A = \epsilon_{CPS}K^* + \epsilon_{CaCPS}K' - \epsilon_{CaCPR} \quad (A13)$$

and a semilogarithmic plot of the quantity $\Theta_{obsd}/[P_T] - \epsilon_{CaCPR}$ vs. time is linear.

References

Agrawal, B. B. L., & Goldstein, I. J. (1967) *Biochim. Biophys. Acta 147*, 262–271.

Alter, G. M., & Magnuson, J. A. (1979) *Biochemistry 18*, 29–36.

Alter, G. M., Pandolfino, E. R., Christie, D. J., & Magnuson, J. A. (1977) *Biochemistry 16*, 4034–4038.

Beckert, W. H., & Sharkey, M. M. (1970) *Int. Arch. Allergy Appl. Immunol. 39*, 337–341.
Bittiger, H., & Schnebli, H. P., Eds. (1976) *Concanavalin A as a Tool*, Wiley, New York.
Brown, R. D., III, Brewer, C. F., & Koenig, S. H. (1977) *Biochemistry 16*, 3883–3896.
Cardin, A. D., & Behnke, W. D. (1978) *Biochim. Biophys. Acta 537*, 436–445.
Cardin, A. D., Behnke, W. D., & Mandel, F. (1979) *J. Biol. Chem. 254*, 8877–8884.
Christie, D. J., Munske, G. R., & Magnuson, J. A. (1979) *Biochemistry 18*, 4638–4644.
Doyle, R. J., Thomasson, D. L., Gray, R. D., & Glew, R. H. (1975) *FEBS Lett. 52*, 185–187.
Edleman, G. M., Cunningham, B. A., Reeke, G. N., Jr., Becker, J. W., Waxdal, M. J., & Wang, J. L. (1972) *Proc. Natl. Acad. Sci. U.S.A. 69*, 2580–2584.
Goldstein, I. J., Hollerman, C. E., & Smith, E. E. (1965) *Biochemistry 4*, 876–883.
Goldstein, I. J., Reichert, C. M., Misaki, A., & Gorin, P. A. J. (1973) *Biochim. Biophys. Acta 317*, 500–504.
Hardman, K. D., & Ainsworth, C. F. (1972) *Biochemistry 11*, 4910–4919.
Harrington, P. C., & Wilkins, R. G. (1978) *Biochemistry 17*, 4245–4250.
Inbar, M., & Sachs, L. (1969) *Proc. Natl. Acad. Sci. U.S.A. 63*, 1418–1425.
Kalb, A. J., & Pecht, I. (1973) *Biochim. Biophys. Acta 303*, 264–268.
Koenig, S. H., Brewer, C. F., & Brown, R. D., III (1978) *Biochemistry 17*, 4251–4260.
Lis, H., & Sharon, N. (1973) *Annu. Rev. Biochem. 42*, 541–574.
Powell, A. E., & Leon, M. A. (1970) *Exp. Cell Res. 62*, 315–325.
Reeke, G. N., Jr., Becker, J. W., Cunningham, B. A., Gunther, G. R., Wang, J. L., & Edleman, G. M. (1974) *Ann. N.Y. Acad. Sci. 234*, 369–382.
Reeke, G. N., Jr., Becker, J. W., & Edleman, G. M. (1978) *Proc. Natl. Acad. Sci. U.S.A. 75*, 2286–2290.
Richardson, C. E., & Behnke, W. D. (1976) *J. Mol. Biol. 102*, 441–451.
Scatchard, G. (1949) *Ann. N.Y. Acad. Sci. 51*, 660–672.
Sherry, A. D., Buck, A. E., & Peterson, C. A. (1978) *Biochemistry 17*, 2169–2173.
Shoham, M., Yonath, A., Sussman, J. L., Moult, J., Traub, W., & Kalb (Gilboa), A. J. (1979) *J. Mol. Biol. 131*, 137–155.
Stroupe, S. D., & Doyle, R. J. (1980) *J. Inorg. Biol. 12*, 173–178.
Sumner, J. B., & Howell, S. F. (1936) *J. Biol. Chem. 115*, 583–588.
Tanford, C. (1967) *Physical Chemistry of Macromolecules*, p 535, Wiley, New York.
Thiers, R. E. (1957) *Methods Biochem. Anal. 5*, 273–335.
Van Holde, K. E. (1973) *Physical Biochemistry*, p 62, Prentice-Hall, Englewood Cliffs, NJ.
Wecksler, M., Levy, A., & Jaffe, W. (1968) *Acta Cient. Venez. 19*, 154–155.
Yariv, J., Kalb, A. J., & Levitzki, A. (1968) *Biochim. Biophys. Acta 165*, 303–305.
Yphantis, D. A. (1964) *Biochemistry 3*, 297–317.